

Design of Superparamagnetic Iron Oxide Nanoparticle for Purification of Histidine-Tagged Recombinant Proteins

Sasmita Mohapatra*, Dibyarupa Pal,** Sudip K. Ghosh** and Panchanan Pramanik*

* Department of Chemistry, IIT Kharagpur, India, 721302, sasmita@chem.iitkgp.ernet.in,
pramanik@chem.iitkgp.ernet.in

** Department of Biotechnology, IIT Kharagpur, India, 721302, dibya02@yahoo.co.in,
sudip@hijli.iitkgp.ernet.in

ABSTRACT

We report a novel purification system for 6 His-tagged proteins by magnetic affinity separation. We have developed superparamagnetic Fe₃O₄@SiO core-shell particles with immobilized surface iminodiacetate groups to chelate with Ni²⁺. This Ni²⁺ magnetic silica nanoparticle has been shown as an efficient carrier, binder and anchor to obtain his-tagged protein directly from total cell lysate. The structural characteristic of the powders, the size of the particle and aggregates in the colloid and magnetic property have been studied by XRD, HRTEM, FTIR, XPS and VSM studies. Due to high efficiency, cost-effectiveness, bio-compatibility and versatility, these magnetic-silica nanoparticles with specific affinity offered by metal chelation may provide new possibilities in biotechnological applications.

Keywords: Superparamagnetic, Magnetite, Nanoparticle, 6xHis tag Protein, Ni affinity chromatography.

1. INTRODUCTION

The expression of recombinant proteins with histidine fusion tag (6xHis) is widely used to ease their purification from a variety of prokaryotic and eukaryotic expression systems.¹⁻³ Immobilized metal-ion affinity chromatography (IMAC) is one of the simplest and most efficient method for purification of 6xHis-Tagged proteins through single capture step.⁴⁻⁶ Immobilized Metal ion affinity chromatography employs affinity ligand attached solid support to immobilize metal ions that form stable complexes with imidazole and thiol end group of proteins. The most commonly used solid support for IMAC is polymeric bead with covalently bonded nitrilotriacetic acid to immobilize nickel ions (Ni²⁺) and separate recombinant proteins those are expressed with 6xHis tags.^{5,6} Though it is a versatile platform for any expressed protein, it has some limitations like high solvent consumption and long operation time. Magnetic separation has been proven as the suitable viable alternative to overcome many of these limitations. In bio-separation, hydrophilically modified magnetic nanoparticle shows higher binding rate than the conventional polymeric bead due to its high surface-to-volume ratio and good dispersibility in aqueous medium. In a very recent article C. Xung *et al* have reported synthesis and application of nitrilotriacetic acid modified Fe-Pt nanoparticles to be used for purification of 6xHis-

tagged protein through IMAC.⁷ However, synthesis of such magnetic carriers is not cost-effective and follows a complicated synthetic route and hence not convenient to be used in large scale purification of protein. In this context we have developed surface modified superparamagnetic iron oxide based magnetic carrier for purification of such recombinant proteins. In the present article we describe our preliminary study on synthesis of superparamagnetic Fe₃O₄@silica core shell nanoparticles with surface-active iminodiacetate groups, which after chelation with Ni²⁺ can be used as a binder and carrier for 6xHis-Tagged proteins.

2. EXPERIMENTAL

2.1 Synthesis of magnetite-silica core-shell nanoparticles

0.324 g FeCl₃ and 0.274 g FeSO₄.6H₂O were taken 40 ml millipore water under argon atmosphere. 5 ml 25 % NH₃ was injected into it while stirring at 4000 rpm in a mechanical stirrer under continuous argon flow for 1 h. Then 100 ml 0.3 molar trisodium citrate was added to it and again stirred for 30 min at 90° C. The particles were collected using magnetic separator followed by washing with 60 ml (3x20 ml) millipore water and then dispersed in 10 ml millipore water for future use. 4 g of this colloid was again taken in 160 ml CH₃OH and 40 ml H₂O mixture. Under continuous mechanical stirring 3 ml NH₃ solution was injected to it. 2 ml of tetraethyl orthosilicate (TEOS) was then consecutively added and the reaction was progressed for 24 h.

2.2 Synthesis of iminodiacetate functionalized magnetite-silica particles

Iminodiacetate was immobilised on these silica coated iron oxide nanoparticles using the process reported by F. B Anspach to introduce iminodiacetate on silica particles.⁸ The silica coated particles were separated out by using magnetic separator, washed and one fourth of the total amount was again dispersed in 40 ml CH₃OH+ H₂O (4:1) mixture. 1 ml of 3-chloropropyltrimethoxysilane was added to the dispersion and sonicated for 30 min at pH 4. The particles were recovered and dispersed in 50 ml 3 M NaOH containing 3 g of iminodiacetic acid followed by stirring at 60°C for 10 h in argon atmosphere. Particles were recovered by magnetic separator followed by thorough

washing with millipore water and stirred with NiCl₂ (CPTS: NiCl₂= 1:10, molar ratio) for 30 min. Then the recovered particles were washed with 30 ml (3x10 ml) millipore water, dispersed in 10 ml water and stored for further use.

2.3 Protein purification study

Purification of histidine tagged recombinant protein from the total cell lysate was carried out by the Ni²⁺ immobilized magnetic nanoparticle. To demonstrate the use of nanoparticle, recombinant nitroreductase (*ntr*) of human parasite *Entamoeba histolytica* was overexpressed with histidine tag in *E. coli*. The protein expression was induced in *E. coli* by IPTG (Isopropyl thio galactopyranoside) at 37°C. In brief the steps used for protein purification were (i) Magnetic nanoparticles were vortexed to get uniform suspension, (ii) Sonicated cell lysate of 1.5 ml culture were added to 50 or 100 μ l magnetic beads and were incubated at room temperature for 30 minutes, (iii) Magnetic beads were separated by magnetic concentrator and washed thoroughly 3x 1ml wash buffer (50mM sodium phosphate, 300mM NaCl, pH-5.0) to remove all the unbound proteins, (iv) Recombinant protein was eluted by 200 μ l of elution buffer (200 mM imidazole), and (v) The beads were separated by magnetic separator and the supernatant containing the desired protein was collected. To verify whether the affinity and specificity of the recovered beads remains unaffected after elution of the proteins, used beads were washed and equilibrated with 1x PBS buffer and Ni²⁺ ions were recharged. Regenerated beads were reused for protein purification. Commercially available Ni-NTA agarose bead has also been used to compare the efficiency of protein purification. Eluted protein was verified in SDS-PAGE analysis.

3. RESULTS AND DISCUSSION

X-ray diffraction pattern of the final product shows broad peak in between 10-20° is due to the amorphous silica coating. The *d*-values match well with those for standard patterns of magnetite (Fe₃O₄) (JCPDS file no 82-1533). The mean crystallite size calculated from the broadening of each peak using Scherer's formula is found to be 10±1 nm.

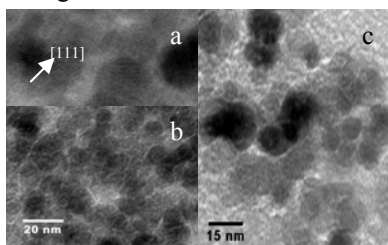


Figure 1 (a) TEM image (b) TEM at high resolution showing lattice imaging of [111] plane (c) TEM image of iminodiacetate functionalized magnetite-silica nanoparticles

Transmission electron micrograph of citrate stabilised magnetite particles (Fig. 1a) shows well dispersed magnetite nanoparticles. Figure 1b shows HRTEM of citrate stabilised magnetite nanoparticles indicating lattice spacing of [111] plane having *d* = 4.9 Å. Particles show narrow size distribution between 5±0.1 nm to 10±0.2 nm with a mean average size of 9.2 nm. Figure 1c presents the TEM image of iminodiacetate functionalized magnetite-silica particles, which shows silica coated particles are almost of uniform size having particle size distribution between 8 nm and 14 nm with mean average particle size of 12 nm.

The comparison of FTIR spectrum of the final product with that of silica coated magnetite and pure iminodiacetic acid gives evidence of immobilisation of IDA on particle surface. Figure 2c shows FTIR spectrum of iminodiacetate immobilised silica spheres. Peaks at 2915, 2856 and 1385 cm⁻¹ indicate the presence of propyl spacer. The peak at 815 cm⁻¹ due to N-H bending in iminodiacetic acid (Fig. 2a) disappears in the spectrum of IDA functionalized magnetite (Fig. 2c) indicating conjugation of IDA on particle surface. A sharp peak at 1627 cm⁻¹ is generated because of asymmetric stretching of -C=O group in 5 membered Ni²⁺-IDA chelate⁸ formed on the surface, which is not observed in case of silica coated magnetite particles before surface functionalisation (Fig. 2b). A broad band between 1300 and 850 cm⁻¹ might be due to overlapping of peaks corresponding to C-N, Si-O-Si stretching vibrations. In case of bulk Fe₃O₄ the vibrational bands of Fe-O appears at 570 and 375 cm⁻¹, however these peaks appear at higher wavenumber, i.e. at 630 and 570 cm⁻¹ in case of IDA functionalized magnetite. This blue shift of absorption band of Fe-O bond can be attributed to quantum sized effect in magnetite nanoparticles. In case of semiconductors it has been verified by many researchers that as the particle size is reduced to approach the exciton Bohr radius there is drastic change in electronic structure and physical properties due to quantum confinement.

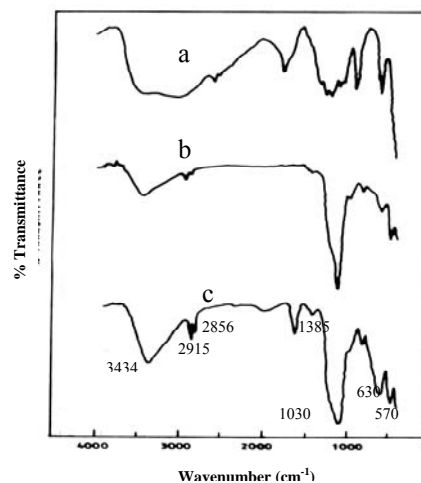


Figure 2. FTIR spectrum of product (a) pure iminodiacetic acid (b) Fe₃O₄@SiO nanoparticles (c) IDA-functionalised Fe₃O₄@SiO nanoparticles

Figure 3 shows X-ray photoelectron spectrum of Ni²⁺ charged iminodiacetate functionalised magnetite-silica nanoparticles under ultrahigh vacuum (UHV) conditions using Al K_α source. C1s spectrum (Fig. 3a) shows three peaks at 285.14, 287.83 and 293.07 eV which account for –CH₂–, C-N and –COOH carbons respectively.^{9,10} The N1s (Fig. 3b) appears at 406.12 eV, which is very close to the N1s binding energy of tertiary nitrogen in Ni-NTA complex¹¹ and hence confirms the immobilization of iminodiacetic acid and magnetic silica nanoparticles. The Ni 2p spectrum shows peaks at 853 and 863 eV attributing to 2p_{3/2} and 2p_{1/2} electrons associated with the corresponding shake-up satellites at 859 and 867 eV. O1s electrons of Fe₃O₄ shows poor XPS signal at 531.5 eV which is obvious as it is present in the core. The broad shoulder of O1s electron at 536 eV can be fitted into three peaks corresponding to oxygen atoms present in three different environments. The intense peak at 536 eV accounts for oxygen present on the silica shell and also for the oxygen through which surface coupling has been obtained. Binding energy corresponding to two types of oxygen present in –COOH, i.e. C=O and C-O appear at 540 and 541.3 eV respectively. Figure 3e corresponds to the binding energy of Fe2p_{3/2} and Fe2p_{1/2} which is consistent with the reported values of Fe₃O₄ in literature.¹²

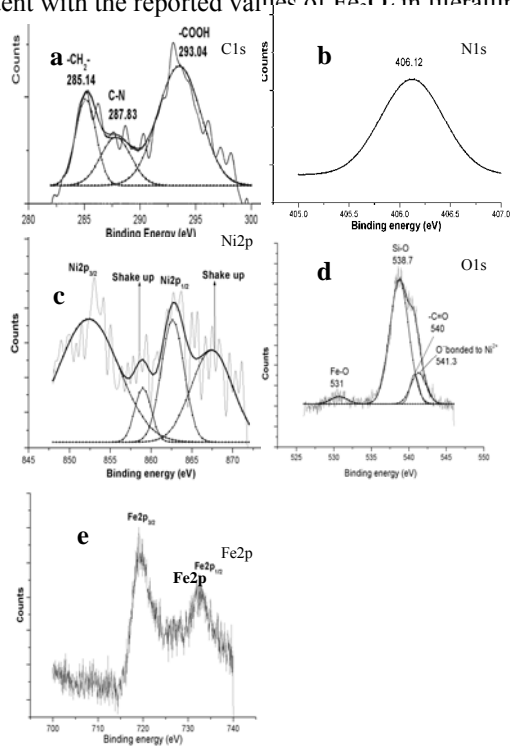


Figure 3. X-ray photoelectron spectra of Ni²⁺ charged magnetite-silica core-shell particles using AlK_α. The solid line shows original curve and dotted line shows the fitted curve **a**) C1s spectrum of along with fit to three peaks described **b**) N1s spectrum which is almost close to that in Ni-EDTA described in literature **c**) Ni2p spectrum along with fit **d**) O1s spectrum along with fit **e**) Fe2p spectrum

Dried nanoparticles were characterized by vibration sample magnetometry at room temperature (Fig. 6). Both uncoated and IDA modified silica coated magnetite particles didn't show any hysteresis and have zero remanence and coercivities at room temperature. The saturation magnetization decreases upon silica coating, which is obvious and consistent with literature.¹³ The decrease in magnetization in functionalized magnetic silica nanoparticles is just the reflection of less magnetic mass in the same.^{14, 15} The consistency in the shapes of the curves further confirms that the decrease in magnetization is primarily due to lower amount of magnetic material per gm rather than any potential magnetic couplings at the interface between the magnetite nanoparticle core and the silica shell.¹³ This superparamagnetism of the synthesized magnetic carriers with high saturation magnetization enables them to exhibit magnetic on-off switching behaviour for which they readily respond and coagulate when exposed to an external magnetic field without any permanent magnetization and again redisperse when the magnetic field is removed.

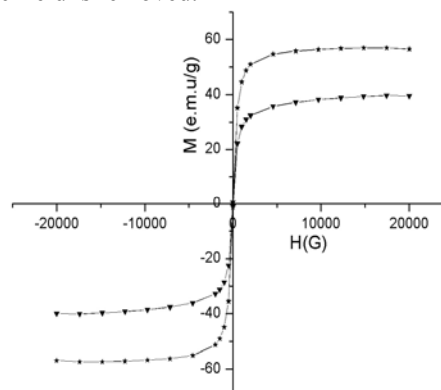


Figure 4. Magnetization curve of citrate stabilized magnetite nanoparticles (marked *) and IDA functionalized magnetic carriers (marked ▲)

Figure 5 presents the SDS-PAGE analysis of the purified recombinant nitroreductase by magnetite-silica nanocarrier. The protein band is visible at about 20 kDa region. After washing the unbound or non-specific proteins on 5 with washing buffer, 6xHis tag nitroreductase was eluted using 200mM imidazole. Single purified protein band of ~20kDa was visualized in SDS-PAGE (Lane 4 and 5, Fig 7). In addition to this, the recovered beads did not lose its affinity for this specific protein when reused (Lane 6, Fig 7). 5 binds to 6xhis-tag proteins at very low protein concentration (15 µg/ml). Furthermore 1.5 mg of protein can be separated using only 1 mg of these superparamagnetic nanoparticles. It indicates the synthesized surface functionalised magnetic particles are more efficient than commercially available magnetic Ni-NTA macrobeads in separating 6xHis-Tagged proteins.

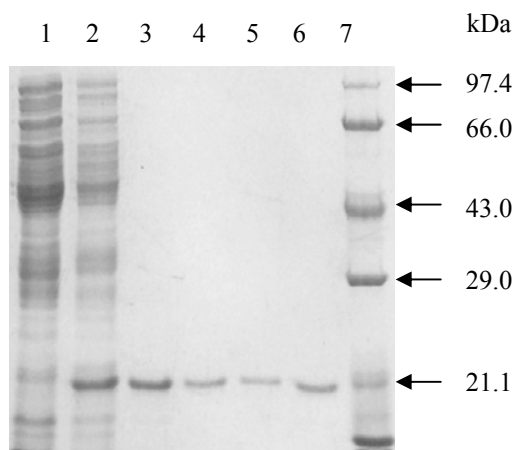


Figure 5 SDS-PAGE analysis of purified recombinant protein by synthesized magnetic nanoparticle. Lane 1, uninduced cell lysate of recombinant protein; Lane 2, induced cell lysate of recombinant protein; Lane 3, eluted fraction by commercially available Ni-NTA beads; Lane 4, eluted fraction with 100µl of magnetic silica beads; Lane 5, eluted fraction by 50µl of magnetic silica beads; Lane 6, eluted fraction by 100µl of reused magnetic silica beads; Lane 7, protein molecular weight marker.

5. CONCLUSION

Superparamagnetic silica coated magnetic nanoparticles of 12 nm with surface iminodiacetate groups have been synthesized and characterized. The immobilisation of Ni²⁺ through the surface affinity ligands has been established using X-ray photoelectron spectroscopy. These Ni²⁺ charged magnetic silica nanoparticles show specific adsorption for 6xHistidine-Tagged recombinant protein. Due to high efficiency, cost-effectiveness, bio-compatibility and versatility, these magnetic-silica nanoparticles with specific affinity offered by metal chelation may provide new possibilities in biotechnological applications.

Reference:

1. J. Schmitt, H. Hess, and H. G. Stunnenberg, *Mol. Biol. Rep.* 18, 223 (1993).
2. A. Hoffman and R. G. Roeder, *Nucleic Acids Res.* 19, 6337 (1991).
3. P. Hengen, *Trends in Biochem. Sci.* 20, 285 (1995).
4. J. Porath, J. Carlsson, I. Olsson, and G. Belfrage, *Nature* 258, 598 (1975).
5. F. H. Arnold, *Nature Biotechnology* 9, 151 (1991).
6. C. F. Ford, I. Suominen, C. E. glatz, *Protein Expr. Purif.* 2, 95 (1991).

7. C. Xu, K. Xu, H. Gu, X. Zhong, Z. Guo, R. Zheng, X. Zhang, and Bing Xu, *J. Am. Chem. Soc.* 126, 3393 (2004).
8. J. A. Neal and N. J. Rose, *Inorg. Chem.* 12, 1226 (1973).
9. S. E. Baker, W. Cai, T. L. Iasseter, K. P. Weidkamp, and R. J. Hamers, *Nano Lett.* 2, 1413 (2002).
10. C. R. Vestal and Z. J. Zhang, *Nano Lett.* 3(12), 1739 (2003).
11. L. Coulier, *Ph. D thesis*, Eindhoven University of Technology, Eindhoven, The Netherlands (2001).
12. S. Liana, Z. Kanga, E. Wanga, M. Jianga, C. Hua, and L. Xua, *Solid State Comm.* 127, 605 (2003).
13. C. R. Vestal and Z. J. Zhang, *Nano Lett.* 3, 1739 (2003).
14. T. Tago, T. Hatsuta, K. Miyajima, M. Kishida, S. Tashiro, and K. Wakabayashi, *J. Amm. Ceram. Soc.* 85, 2188 (2002).
15. F. G. Aliev, M. A. Correa-Duarte, A. Mamedov, J. W. Ostrander, M. Giersig, L. M. Liz-Marzan, and N. A. Kotov, *Adv. Mater.* 11, 1006 (1999).